

Extent, Extremum, and Curvature: Qualitative Numeric Features for Efficient Shape Retrieval

B. Gottfried, A. Schuldt, and O. Herzog

Centre for Computing Technologies (TZI)
University of Bremen, Am Fallturm 1, D-28359 Bremen

Abstract. In content-based image retrieval we are faced with continuously growing image databases that require efficient and effective search strategies. In this context, shapes play a particularly important role, especially as soon as not only the overall appearance of images is of interest, but if actually their content is to be analysed, or even to be recognised. In this paper we argue in favour of numeric features which characterise shapes by single numeric values. Therewith, they allow compact representations and efficient comparison algorithms. That is, pairs of shapes can be compared with constant time complexity. We introduce three numeric features which are based on a qualitative relational system. The evaluation with an established benchmark data set shows that the new features keep up with other features pertaining to the same complexity class. Furthermore, the new features are well-suited in order to supplement existent methods.

1 Introduction

Content-based retrieval from large image databases is a challenging problem in computer vision. Its importance grows continuously with the increasing penetration of image databases in many areas of everyday life. As an example, think of Flickr¹, which is an internet platform for uploading and sharing of photographic content. Large amounts of image data can also be found in the economic as well as the scientific area. The pure amount of content, and even more its fast growth, illustrates the demand for efficient and effective search strategies. Therefore, it is particularly desirable to choose features with only little computational complexity for the comparison of images. In image retrieval, this has already been applied for a long time to colour and texture. As an example, think of colour histograms having a fixed number of entries. Consequently, they can be compared with constant time complexity.

For the comparison of objects by their shape there exist also meaningful methods [9]. However, their efficiency in terms of computational complexity is still a problem. As an example, the approach of [8] which achieves promising retrieval results has a biquadratic time complexity, $O(n^4)$. This is different for

¹ <http://www.flickr.com/>

numeric shape features [3, 4]. They characterise shapes by a single numeric value. This entails two advantages: First, two shapes described by such a feature can be compared with constant time complexity, $O(1)$. Second, the shapes of an image database can be ordered in accordance to a numeric shape feature. This allows retrieval algorithms to be applied which employ binary search strategies with a time complexity of $O(\log n)$, with n being the number of images in the database.

Applied exclusively, however, the retrieval performance for each of these features is rather limited since each one describes only one simple property of an object, e.g. the aspect ratio [3] of the minimal enclosing rectangle. But combining such simple features improves classification results significantly, still with constant time complexity for the comparison of two shapes. Characterising an object twice by similar features, however, does most likely not improve its description. By contrast, it is more promising to combine features which are built upon different foundations. We introduce three new numeric shape features based on a qualitative approach, thereby complementing existing features. Afterwards, we combine them with existing quantitative numeric shape features.

The remainder of this paper is structured as follows: In Sect. 2 we introduce previous work that underlies our new approach which is then presented in Sect. 3. We evaluate our method in Sect. 4 by comparing it to other approaches. Eventually, a conclusion follows in Sect. 5.

2 Previous Work

The work presented in this paper focuses on the characterisation of shapes. For this purpose, it is assumed that silhouettes have been segmented from raster images before. Contours of silhouettes can then be represented by polygons, as it has been motivated from the cognitive point of view by [2]. Additionally, the following reasons support a pure cognitive motivation: First of all, confining oneself to contour points the uniform distribution of points of the silhouette's interior can be excluded. Since only the contour points are relevant concerning any object's outer shape, this restriction does not entail any loss of relevant information. Secondly, the application of polygonal approximation algorithms [11] allows a massive data reduction with only little influence on the perception of shape. We apply especially the method of [10], thereby choosing a scale-invariant approximation error of one percent of a polygon's perimeter.

2.1 Reference System

The polygon obtained in the previous step of abstraction forms a quantitative description of the underlying shape. The concrete representation depends on scale, translation, and rotation of the object under consideration. Furthermore, it is imprecise due to noise in the underlying image data. The aim is therefore to achieve an invariance against scale, translation, and rotation as well as a certain robustness against noise.

In order to meet the above objectives we apply the orientation grid of [15] which brings in a qualitative abstraction. It is induced by each of the polygon's line segments as depicted in Fig. 1 (after an orientation has been imposed on the polygon) and it consists of three auxiliary lines. The first one runs through the reference segment allowing the qualitative distinction whether a point is located on its left or right hand side. The two other lines are oriented orthogonally to the first one, whereby each of them passes either the reference segment's start point or its end point. Their arrangement enables the decision whether a point lies in front of the reference segment, next to, or behind it. In general, the orientation grid divides the two-dimensional plane into six sectors, as depicted on the left hand side of Fig. 1. Instead of its quantitative coordinates it is then possible to characterise a point by its position relative to the respective line segment. This is the third sector in the example depicted in the centre of Fig. 1. This description is invariant against scale, translation, and rotation since the orientation grid is an intrinsic reference system of the polygon, i. e. it is induced on each of its line segments. A certain robustness against noise is achieved by partitioning the two-dimensional plane into sectors. Generally, changing a point's quantitative position does not change the sector it is located in; even larger movements of points only result in neighbouring sectors.

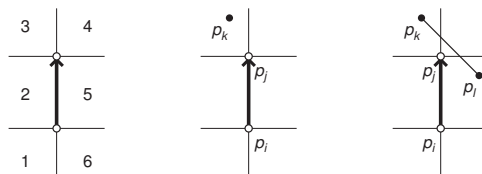


Fig. 1. Left: The orientation grid divides the two-dimensional plane into six sectors. Centre: The qualitative position of p_k is in sector 3, which is located front left w. r. t. the reference line $\overline{p_i p_j}$. Right: The line segment $\overline{p_k p_l}$ passes the sectors 3, 4, and 5

2.2 Bipartite Arrangements

Apart from characterising single points it is also possible to apply the orientation grid in order to relate two polygonal line segments to each other. This is achieved by the qualitative concept of bipartite arrangements [5, 6], in short \mathcal{BA} . The extension from characterising single points to line segments is straightforward. As each line segment is defined by a start and an end point, these points have to be taken into consideration. Both of them can be located in any of the six sectors of the orientation grid (Fig. 1 right). Hence, this theoretically leads to a number of $6^2 = 36$ conceivable arrangements between two line segments. By omitting symmetries and intersections [5] it is possible to reduce this number to those 23 \mathcal{BA}_{23} relations that are depicted on the left hand side of Fig. 2. Their mnemonic labels are given in the centre of the same figure. As this approach relates line

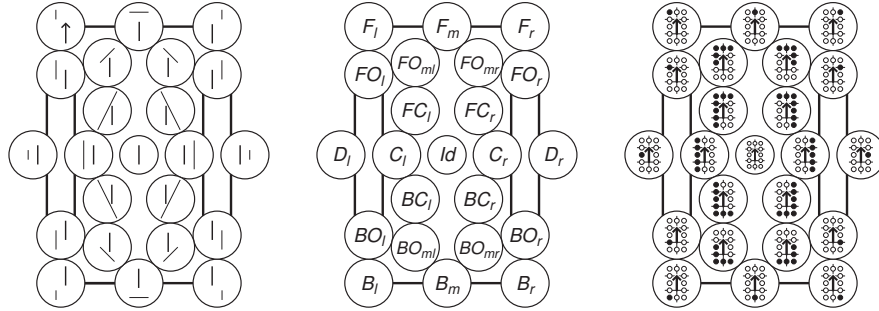


Fig. 2. Example configurations (left) and mnemonic labels (centre) for the 23 \mathcal{BA}_{23} relations between two line segments in the two-dimensional plane. Right: The iconic representation of the bipartite arrangement's scopes

segments in the two-dimensional plane it can be categorised as an extension of Allen's 13 qualitative relations between one-dimensional intervals [1].

A bipartite arrangement relation describes the position of a line segment w. r. t. a reference segment. A polygon's whole course can then be characterised by applying a sequence of \mathcal{BA}_{23} relations, describing each of the n polygonal line segments, one after another [6]:

Definition 1 (Course) *Let x be a line segment of a simple, closed polygon. Its course, in short $C(x)$, contains the \mathcal{BA}_{23} relations of all segments y_i w. r. t. x :*

$$C(x) := (x_{y_0}, \dots, Id, \dots, x_{y_{n-1}}), x_{y_i} \in \mathcal{BA}_{23}; i = 0, \dots, n - 1$$

Hence, we obtain a qualitative description of the considered polygon w. r. t. one of its segments. In order to arrive at a complete description it is necessary to apply not only one line segment as a reference, but all of them, one after another. This results in the following definition:

Definition 2 (Polygonal Course) *Let P be a simple, closed polygon. Its polygonal course, in short $C(P)$, is the conjunction of all courses of P :*

$$C(P) := \bigwedge_{i=0}^{n-1} C(x_i)$$

The result is a matrix that comprises all n^2 \mathcal{BA}_{23} relations that exist between the polygon's n line segments.

2.3 Scopes of Bipartite Arrangements and Courses

Based on the work of [5, 6] a more general approach has been introduced by [12, 13]. Their idea is to represent \mathcal{BA}_{23} relations and even courses as sets of atomic relations. The advantage of such a representation is that it allows to apply standard set operations, e. g. union and intersection. A \mathcal{BA} is considered atomic if

it populates only one of the orientation grid’s sectors, which holds for B_l , D_l , F_l , F_r , D_r , as well as B_r (Fig. 2 left). Furthermore, those relations connecting adjacent sectors, namely BO_l , FO_l , F_m , FO_r , BO_r , and B_m , are also atomic. Altogether, these twelve relations form $\mathcal{BA}_{12} \subset \mathcal{BA}_{23}$.

Each \mathcal{BA}_{23} relation can then be represented by its *scope*, i. e. the set of atomic relations it consists of. The right hand side of Fig. 2 visualises the \mathcal{BA}_{23} relations’ scopes. Each of the twelve circles stands for the atomic relation that is located at its position in the orientation grid. An opaque circle thereby means that the atomic relation is part of a scope, while a transparent one indicates its absence. This results in the following definition:

Definition 3 (Scope of a \mathcal{BA}) *Let x and y be line segments of a simple, closed polygon. The set of atomic \mathcal{BA}_{12} relations that represents the relation $x_y \in \mathcal{BA}_{23}$ is called the relation’s scope, in short $\sigma(x_y)$:*

$$\sigma(x_y) := \{x_{y_1}, \dots, x_{y_n}\}, x_{y_i} \in \mathcal{BA}_{12}$$

Each scope is a description with constant space complexity as the total number of atomic relations that may be contained in a scope is limited to $|\mathcal{BA}_{12}| = 12$. While a single \mathcal{BA}_{23} relation is limited to characterising the relationship between two line segments, this limitation does not hold for scopes. By contrast, it is also possible to characterise the position of a whole course by a single scope relation. This can be achieved by exploiting the scope’s set property. In particular, we create the union of the scopes of all \mathcal{BA}_{23} relations participating in a course:

Definition 4 (Scope of a Course) *Let x be a line segment of a simple, closed polygon and $C(x)$ its course. The set of atomic relations describing the position of $C(x)$ is called the scope of the course, in short $\sigma(C(x))$:*

$$\sigma(C(x)) := \bigcup_{i=0}^{n-1} \sigma(r_i), r_i \in \mathcal{BA}_{23}$$

Proceeding this way, however, leads to a certain loss of information since Gestalt features are not further considered within the scope of a given course. Nevertheless, the resulting characterisation offers still the expressiveness for applying concepts such as the scope histogram [13] which computes the frequencies of a polygon’s scopes, leading to promising results as has been shown in [12].

3 Qualitative Numeric Shape Features

The scope histogram [13] forms a very compact representation as it characterises the shape of an object with constant space complexity. It is a statistical shape descriptor as it considers only the frequencies with which the courses’ scopes occur. The notion of scope, however, is not limited to statistics. By contrast, it is also possible to derive further compact shape features from a polygonal course (Definition 2). In this section we particularly introduce three of them, namely the numeric shape features *extent*, *extremum*, and *curvature*, which are defined on the basis of the scope approach.

3.1 Extent

The notion of a course (Definition 1) can be applied in order to characterise a polygon qualitatively w. r. t. its line segment x . Definition 4 introduces the so-called scope of a course as a more compact representation. By applying a set of atomic \mathcal{BA}_{12} relations the scope $\sigma(C(x))$ specifies which of the orientation grid's sectors are populated by the given course. In general, the complexity of a shape increases with the number of orientation grid sectors that are passed by its course. This observation leads to the definition of the extent, which is a simple measure of a shape's complexity. The number of populated sectors correlates with the atomic relations within the respective scope. Thus, it is sufficient to count the atomic relations a scope comprises (Fig. 3). The maximum range η_{\max} of an extent η is defined by the maximally possible number of atomic relations within a scope, which is $\eta_{\max} = |\mathcal{BA}_{12}| = 12$. This results in the following definition:

Definition 5 (Extent) *Let x be a line segment of a simple, closed polygon and $\sigma(C(x))$ the scope of its course. The number of the atomic \mathcal{BA}_{12} relations of the scope is called the extent of the scope, in short $\eta(\sigma(C(x)))$, and it holds that*

$$\eta(\sigma(C(x))) := |\sigma(C(x))| \in \{1, 2, \dots, \eta_{\max}\}$$

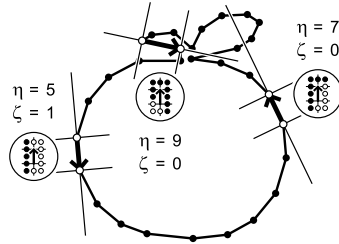


Fig. 3. An apple. The three highlighted reference segments demonstrate the computation of extent η and extremum ζ from the respective line segments' scopes

Definition 5 determines the extent of a single course. This extent characterises the complexity of a polygon as perceived by the line segment on which the orientation grid is currently induced. However, as mentioned before each polygon is characterised by n courses, where n is the total number of line segments. We obtain a single numeric value, that characterises the whole polygon, by computing the average extent for all courses. In order to arrive at a normalised value in $[0, 1]$, the polygonal extent is divided by η_{\max} :

Definition 6 (Polygonal Extent) *Let P be a simple, closed polygon. Its polygonal extent, in short $\eta(P)$, is the average number of the atomic \mathcal{BA}_{12} relations of the scopes of all courses $C(x_i)$ of P :*

$$\eta(P) := \frac{1}{n \eta_{\max}} \sum_{i=0}^{n-1} \eta(C(x_i))$$

Figure 4 depicts example silhouettes from the database of [9] that illustrate the range of possible extents η . The spring at the top left position exhibits the highest extent. This is due to the line segments that are located within the spring's ends. Their extent is maximal, i.e. $\eta_{max} = 12$, since the course of these segments runs completely around them. The extent of the depicted objects decreases from the top left to the bottom right. Out of all objects the triangle has the lowest extent: for each of its line segments the polygon is solely located in the second sector of the orientation grid, i.e. $\eta = 1$. These examples demonstrate that the extent of a shape can easily be comprehended. Generally spoken, the extent is the higher the more complex the underlying shape is, in terms of indentations and how complex they are shaped.

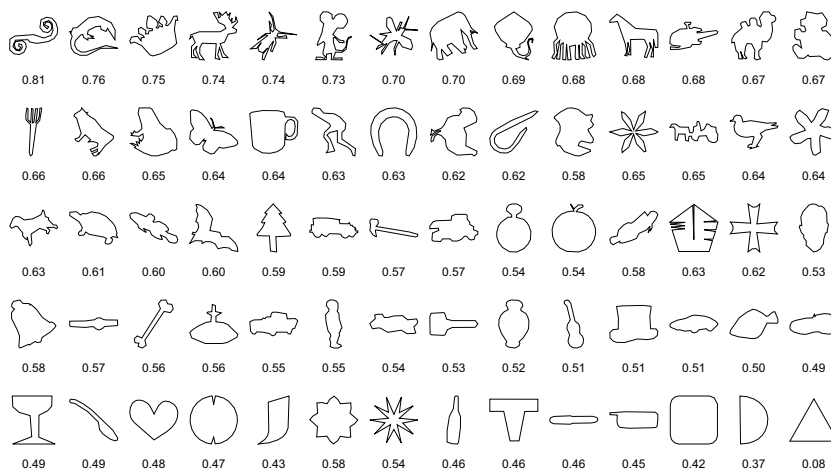


Fig. 4. Example shapes ordered accordingly to their extent η

3.2 Extremum

The second qualitative shape feature that can be derived from the scope is called the extremum. It tells us for a given line segment whether it is an extremum of its respective polygon. Thereby, we denote a line segment as extreme if it is part of the polygon's convex hull. This in turn is the case whenever no other part of the polygon is located on the right hand side of the considered line segment. Detecting such a configuration on the basis of the scope representation is fairly straightforward: in this case the whole polygon is l , i.e. it is located left w.r.t. the reference segment. One possibility to realise l is the scope $\sigma(C_l)$ of the \mathcal{BA}_{23} relation C_l (Fig. 2).

Proposition 1 (Extremum) *Let x be a line segment of a simple, closed polygon. x is said to be an extremum, in short $\zeta(C(x))$, if*

$$\zeta(C(x)) = \begin{cases} 1 & \text{iff } \eta(\sigma(C(x)) \cup l) = \eta(l) \\ 0 & \text{else} \end{cases}$$

Proof: A union between l and a scope $\sigma(C(x))$ of a course $C(x)$, that leads to an increase in the scope's extent, means that further atomic relations have been added by means of the union operation. As the scope l already contains all atomic relations on the reference segment's left hand side, the additional atomic relations must lie on its right hand side. \square

From the three example line segments highlighted in Fig. 3 only the leftmost one is extreme. It is the only one that comprises atomic relations solely on its left side. The other scopes' atomic relations populate both halves of their respective orientation grids. In order to obtain a characterisation of the whole polygon, we count the extreme segments and relate them to the number of line segments contained in the polygon:

Definition 7 (Polygonal Extremum) *Let P be a simple, closed polygon. Its polygonal extremum, in short $\zeta(P)$, measures, how many segments of P are extremes:*

$$\zeta(P) := \frac{1}{n} \sum_{i=0}^{n-1} \zeta(C(x_i))$$

Figure 5 shows example silhouettes in conjunction with their respective extremum values. Since they are completely convex the first three objects (a square, a triangle, and a semi circle) have the highest extremum values. The number and size of concavities increase from the top left to the bottom right. None of the line segments of the last three devices is convex. Consequently, the extremum values of these shapes are zero. Therewith, the ordering established by the extremum corresponds to the visual perception of the considered shapes' convexity.

3.3 Curvature

The third feature we shall introduce here is referred to as the curvature. It describes how often the course $C(x)$ changes its position as perceived from its reference segment x . More specifically, it is examined how often the relations within the course change from one atomic \mathcal{BA}_{12} relation to another one. For this purpose, it is not sufficient to analyse the scope $\sigma(C(x))$ of the course $C(x)$ as a whole. It is rather necessary to analyse the scope of every single relation in $C(x)$ in order to relate it to its successor:

Definition 8 (Curvature) *Let x be a line segment of a simple, closed polygon and $C(x)$ its course. The curvature of $C(x)$, in short $\xi(C(x))$, arises from the*

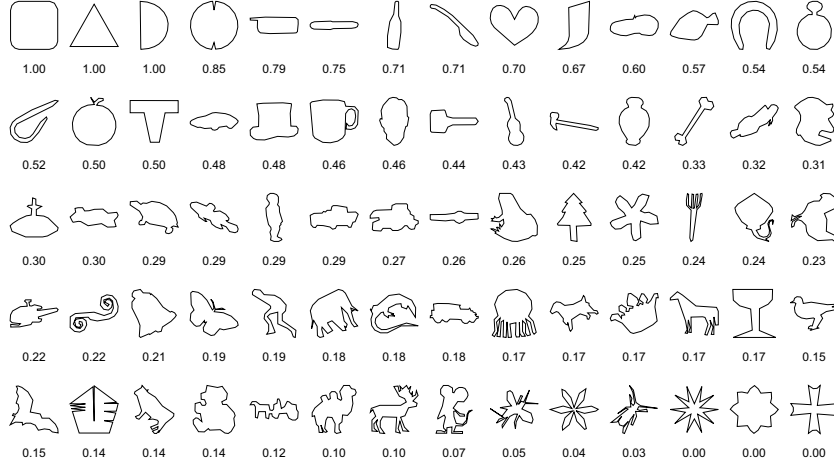


Fig. 5. Example shapes ordered accordingly to their extremum ζ

sequence of its relations r_i as follows:

$$\xi(C(x)) := \sum_{i=0}^{n-1} \begin{cases} 0 & \text{if } r_i = Id \wedge (str(r_i) \wedge int(r_{i-1}, r_{i+1})) \\ 1 & \text{if } r_i = Id \wedge (str(r_i) \vee int(r_{i-1}, r_{i+1})) \\ 2 & \text{if } r_i = Id \\ \eta(\sigma(r_i)) - 1 & \text{if } int(r_i, r_{i+1}) \\ \eta(\sigma(r_i)) & \text{else} \end{cases}$$

The first three cases in Definition 8 occur when the currently considered segment is the reference segment itself. Before discussing these special cases, we shall start with an analysis of the more general cases, namely the fourth and the fifth one.

The right hand side of Fig. 2 depicts the distinguishable scopes for single line segments. Some of these scopes contain more than one atomic relation, which means that a change of position w. r. t. the reference segment already occurs within the respective line segment. The total number of changes in position is thereby defined by the extent of the scope of one line segment's relation: $\eta(\sigma(r_i)) - 1$. Another change in position may occur between two subsequent line segments r_i and r_{i+1} . However, this is only the case, if their scopes do not intersect, i. e. they have no atomic relation in common. In order to determine such an intersection, we apply an auxiliary function. It creates the intersection of the scopes under consideration. The intersection is not empty if the result's extent is greater than zero:

$$int(r_1, r_2) := \begin{cases} \text{true} & \text{iff } \eta(\sigma(r_1) \cap \sigma(r_2)) > 0 \\ \text{false} & \text{else} \end{cases} \quad (1)$$

We shall now address the special case in which the considered line segment is the course's reference segment itself. In this case it does not suffice to examine

the intersection in the scopes of the predecessor and the successor. It is additionally necessary to find out whether or not the course has a kink around this segment. Therefore, the reference segment's predecessor and successor have to be compared. If the scope σ of one relation is the inverse σ^{-1} of the other one, the course has no kink. This can be determined using the following auxiliary function:

$$str(r_i) := \begin{cases} \text{true} & \text{iff } \sigma(r_{i-1}) = \sigma^{-1}(r_{i+1}) \\ \text{false} & \text{else} \end{cases} \quad (2)$$

Figure 6 gives an example on the application of the two auxiliary functions with which we are now able to determine the curvature for a single course. However, in order to compute the curvature for a whole polygon, we have to extend our definition again. Therefore, the average curvature for all of the polygon's n courses is determined. The range of the curvature for a single course is thereby $[1, \infty[$. In order to arrive at a value in $]0, 1]$ like for the other features, we compute each curvature's multiplicative inverse:

Definition 9 (Polygonal Curvature) *Let P be a simple, closed polygon. Its polygonal curvature, in short $\xi(P)$, is defined as the average of the multiplicative inverses of the curvatures of all courses $C(x_i)$ of P :*

$$\xi(P) := 1 - \frac{1}{n} \sum_{i=0}^{n-1} \frac{1}{\xi(C(x_i))}$$

The curvature values of example silhouettes are given in Fig. 7. The object that is most curved is the spring on the left hand side. The curvature decreases from the top left to the bottom right. The triangle exhibits the lowest curvature. That is, as in the case of the extremum and extent, also the curvature corresponds with the visual perception of the silhouettes: the more curved an object is the higher its qualitative curvature value is.

3.4 Comparison

Figures 4, 5, and 7 illustrate, that convex shapes (high extremum values) coincide with low values for extent and curvature. Thus, there seems to be a correlation of extremum with both extent and curvature. The correlation observed between extremum and extent can be explained by the fact that convex shapes are only located left w. r. t. their polygon which also restricts the range of their extent. Furthermore, convex shapes are bent only into one direction. Since they comprise no reversals also the range for their curvature is limited. These correlations indicate why a combination of these three features will most likely not be as effective as a combination of completely independent features.

However, our new features are by no means completely redundant. On the contrary, there exist also situations in which our new features supplement each other. One counter-example against the correlation is formed by the pencil and the triangle on the left hand side of Fig. 8. While both of them are completely

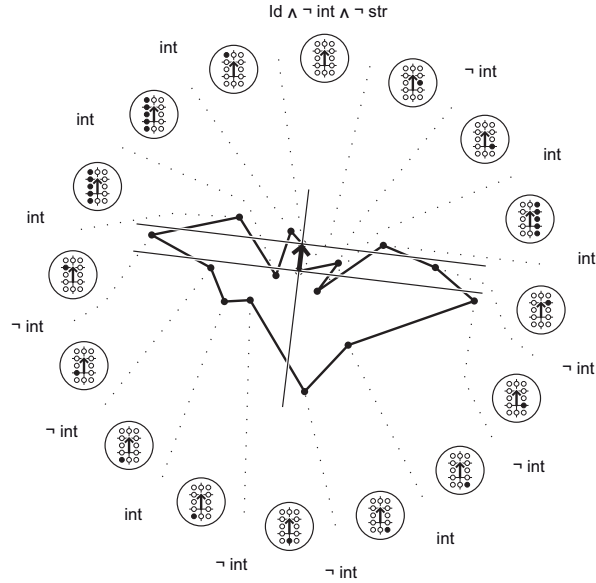


Fig. 6. A bat. All line segments' scopes w. r. t. the highlighted reference segment. The result of the auxiliary functions is denoted for each pair of consecutive line segments. The curvature ξ of this example course is 21

convex (i.e. have an extremum of 1.0) they can still be distinguished by their extent and curvature. The right hand side of Fig. 8 depicts two silhouettes which exhibit the same curvature, but nevertheless differ in their extent and extremum values. This is due to the fact that the right polygon comprises some convex line segments (those lying on the convex hull, i.e. being extreme according to Definition 1) while the left one has none of them (relating to the extremum values). Furthermore, the right hand side polygon is much more folded than the left hand polygon (relating to its higher extent).

4 Retrieval Performance

In order to assess the retrieval performance of our approach we shall now conduct an evaluation. As introduced above our method focuses on the shape of objects. Hence, we apply particularly the popular core experiment CE-Shape-1 [9] for the MPEG-7 standard. The purpose of this experiment is to compare different shape descriptors. It takes only retrieval results into account, thereby completely abstracting from the underlying algorithms. Thus, it allows our shape features to be measured in comparison with others that have already been examined with this standardised reference test.

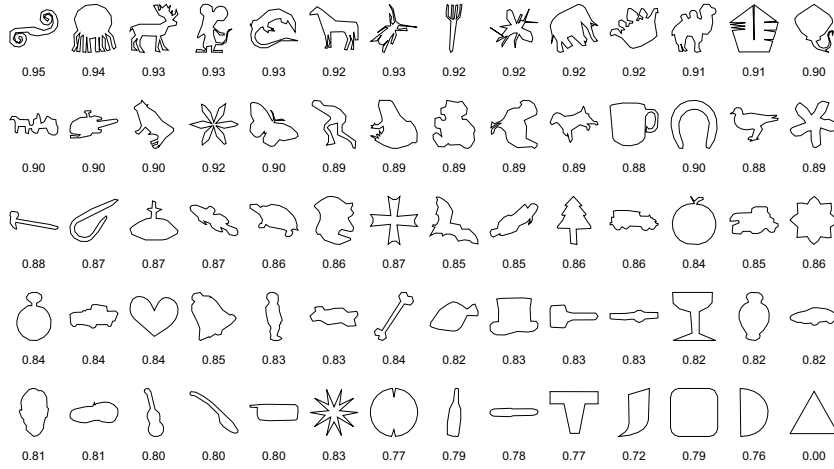


Fig. 7. Example shapes ordered accordingly to their curvature ξ



Fig. 8. Left: Two convex shapes with same extremum ζ that can nevertheless be distinguished by their extent η and curvature ξ . Right: Two shapes with same curvature values ξ , but different extent η and extremum ζ

4.1 Experiment

We especially focus on Part B of the reference test which addresses similarity-based shape retrieval. The experiment comes along with a database of 1400 silhouette images. These images are grouped together into 70 classes, whereby each class comprises 20 instances. Figures 4, 5, and 7 depict example instances of all 70 classes. During the test each image serves as a query, one after another. All others are ordered concerning their similarity according to the approach under consideration. The test's result is determined accordingly to the following definition: For each query, the correct matches among the first 40 results are counted. This number is then related to the maximally possible number of correct results. This is 20 for each single query (since each class comprises 20 instances) and 28000 for all 1400 queries. Thus, a result of 100% means that all expected results are found. Nevertheless, such an outcome is most unlikely if only shape knowledge is applied [9]. This is due to the fact that the 70 classes are grouped by semantic aspects, which means that some of them exhibit a broad bandwidth of different shapes. Conversely, using a hypergeometric distribution, it is easy to show that a random ordering of the search results achieves about 2.86% in the MPEG test. This is a lower bound showing how much better an approach is in comparison with mere chance.

4.2 Existing Approaches

Our new shape features are confined to a single numeric value. This allows a comparison with constant computational complexity. Hence, it is a good choice to compare them to approaches exhibiting the same complexity. We consider three quantitative numeric shape features. These are the compactness [3], which is the ratio $\frac{4\pi A}{P^2}$ of a polygon’s area and perimeter, and the radius ratio [4] $\frac{R_{min}}{R_{max}}$ of the minimum enclosing circle and the maximal contained circle. Furthermore, we apply the aspect ratio [3] $\frac{H_r}{W_r}$ of the minimal enclosing rectangle. These three features have in common that they are based on fundamental geometric properties and that they represent a shape by just one single number.

Apart from the above numeric features, we compare our method also to two other approaches which also pertain to the same class of complexity. On the one hand the seven invariant Hu moments [7], which can directly be applied to polygons [14], on the other hand the scope histogram of [12], which is based on the scope of polygons like our method. In contrast to our approach which determines visual shape properties, the scope histogram simply computes how often the 86 distinguishable scopes occur in a polygon.

4.3 Retrieval Results

The classification results of our new numeric shape features compared to the previous ones can be found in Table 1. The results show that all numeric features separately achieve results between about 16% and 25%. Thereby, our new qualitative features slightly outperform the quantitative ones. All considered numeric features clearly exceed the 3% of a random ordering five to eight times. This is notable since each feature consists of only one single numeric value. The Hu moments and the scope histogram achieve better results of about 34% and 46% respectively. This, however, is not surprising as they comprise a more complex range of distinctions, namely seven and 86 respectively.

Table 1. Retrieval results of the numeric shape features extent (ET), extremum (EM), curvature (CU), compactness (CO), radius ratio (RR), and aspect ratio (AR) examined with CE-Shape-1 Part B. Furthermore, also the Hu moments (HU) as well the scope histogram (SH) are evaluated

ET	EM	CU	CO	RR	AR	HU	SH
24.97	18.19	23.30	21.86	16.82	24.12	34.13	45.52

Owing to their low computational complexity, it is possible and reasonable to combine multiple numeric features. This, however, only makes sense if the results are improved by such combinations. The classification results of these combinations are summarised in Table 2. Our new qualitative numeric features

achieve a retrieval result of about 34%. This is already remarkable as they slightly outperform the seven Hu moments. Nevertheless, their result lies below 52% achieved by the three quantitative numeric features. This can be explained by the fact that all qualitative features are based on the scope (see Sect. 3.4), while the quantitative ones base on different geometric properties. Together, all six numeric features achieve a retrieval result of about 62%. This is especially remarkable as we apply only six numeric values for the characterisation of the objects' shapes, i. e. we only need constant time for the comparison of two shapes. Especially, the result of the quantitative numeric features combined with the Hu moments lies about eight percentage points below their combination with our new features. The quantitative numeric features and the scope histogram slightly outperform the combination of the six numeric features. However, the scope histogram consists of 86 numeric values while we apply only six of them.

Table 2. Combining multiple numeric features improves the retrieval results: the qualitative features (QL), the quantitative features (QN), as well as the combination of all numeric features (AN). For comparison, the quantitative features have also been combined with the Hu moments (NH) and the scope histogram (NS)

QL	QN	AN	NH	NS
34.33	51.58	61.51	53.99	63.75

From the low computational complexity of $O(1)$ results a fast execution. On a computer with Windows XP and an Intel Centrino Duo processor with 2.16 GHz it takes only about five seconds in order to conduct the whole MPEG test (nearly two million comparisons) for the six numeric shape features. Eventually, it is worth mentioning that a classification result of 62% is only about 15 percentage points less than the approach of [8] who achieve 76.45%. However, their computational complexity is biquadratic while ours is still constant.

5 Conclusion

In this paper we introduce extent, extremum, and curvature, three new numeric shape features. While other numeric shape features directly base on geometric properties, we apply a polygonal approximation as well as a qualitative abstraction before. The orientation grid as an underlying intrinsic reference system brings in an invariance against scale, translation, and rotation. Furthermore, the polygonal approximation and the coarse perspective of the qualitative representation realise a certain robustness against noise in the underlying image data. The new features are easily comprehensible as they are defined on the qualitative relational system of the scope approach.

The evaluation results show that our new numeric features can keep up with comparable methods. The retrieval performance can be improved by combining

multiple numeric features. Together with the three quantitative numeric features discussed in this paper a retrieval result of about 62% in the MPEG test is achieved. Hence, the new features in fact supplement the other established features. Other features pertaining to the same complexity class can thus be outperformed. The retrieval result is remarkable as only six numeric values are applied for the characterisation of each shape. The computational complexity for the comparison of two of these shapes is therefore constant. The achieved result is only about 15 percentage points less than the 76.45% of [8]. However, their computational complexity is biquadratic while ours is constant.

References

1. J. F. Allen. Maintaining Knowledge about Temporal Intervals. *Communications of the ACM*, 26(11):832–843, 1983.
2. F. Attneave. Some Informational Aspects of Visual Perception. *Psychological Review*, 61:183–193, 1954.
3. R. O. Duda and P. E. Hart. *Pattern Classification and Scene Analysis*. John Wiley & Sons, 1973.
4. G. D. Garson and R. S. Biggs. *Analytic Mapping and Geographic Databases*. Sage Publications, 1992.
5. B. Gottfried. Reasoning about Intervals in Two Dimensions. In *IEEE Int. Conf. on Systems, Man and Cybernetics*, pages 5324–5332, The Hague, The Netherlands, 2004.
6. B. Gottfried. *Shape from Positional-Contrast — Characterising Sketches with Qualitative Line Arrangements*. Deutscher Universitäts-Verlag, 2007.
7. M.-K. Hu. Visual Pattern Recognition by Moment Invariants. *IRE Transactions on Information Theory*, 8(2):179–187, 1962.
8. L. J. Latecki and R. Lakämper. Shape Similarity Measure Based on Correspondence of Visual Parts. *IEEE PAMI*, 22(10):1185–1190, 2000.
9. L. J. Latecki, R. Lakämper, and U. Eckhardt. Shape Descriptors for Non-rigid Shapes with a Single Closed Contour. In *IEEE CVPR*, pages 424–429, Hilton Head Island, SC, USA, 2000.
10. D. A. Mitzias and B. G. Mertzios. Shape Recognition with a Neural Classifier Based on a Fast Polygon Approximation Technique. *Pattern Recognition*, 27:627–636, 1994.
11. P. L. Rosin. Assessing the Behaviour of Polygonal Approximation Algorithms. *Pattern Recognition*, 36:505–518, 2003.
12. A. Schuldt, B. Gottfried, and O. Herzog. Retrieving Shapes Efficiently by a Qualitative Shape Descriptor: The Scope Histogram. In *CIVR 2006*, pages 261–270, Tempe, AZ, USA, 2006.
13. A. Schuldt, B. Gottfried, and O. Herzog. Towards the Visualisation of Shape Features: The Scope Histogram. In *KI 2006*, pages 289–301, Bremen, Germany, 2006.
14. C. Steger. On the Calculation of Arbitrary Moments of Polygons. Technical Report FGBV-96-05, Informatik IX, Technische Universität München, 1996.
15. K. Zimmermann and C. Freksa. Qualitative Spatial Reasoning Using Orientation, Distance, and Path Knowledge. *Applied Intelligence*, 6:49–58, 1996.